On the internal structure of piezo-electric devices: Closed and Open Loop Optimal Strategies

ANDRES G. GARCIA, LUCIANO PONS AND EMANUEL PEROTTI
Grupo de Investigación en Multifísica Aplicada (GIMAP)
Universidad Tecnológica Nacional
11 de Abril 461
ARGENTINA
andresgarcia@frbb.utn.edu.ar

Abstract: - Piezo-electric devices possess the ability to produce high voltages without load. However, to harvest this energy, the complex and capacitive internal structure must be deal with. This capacitive behavior makes the AC-DC conversion too involved. If a buck-boost topology is to be designed to regulate the DC output, the discontinuous mode provides constant input impedance for small amount of power. However, the input impedance of a buck-boost is a function of the switching frequency and inductance, bounding the maximum values. This open-loop strategy is adequate for small size PCB applications, for instance in energy harvesting applied to sensors, whereas, closed-loop and optimal control algorithms will improve the output power. In this paper a closed-loop optimal control algorithm to work with any source of electrical input voltage in a buck-boost converter is considered. This optimal control yields a much bigger output power when compared to the case of non-optimal control. With piezo-electric devices, the output power harvested shows a significant improvement, thus mitigating their natural drop in open loop. Some simulations as well as comparisons with real measurements using two different kind of commercial piezo-electric devices are presented. On the other hand, the internal structure of piezo-electric generators is explored using an open loop optimal control strategy along with an intermediate active circuit. Following the reading of the measurements and the theory developed in this paper, conclusions and future work are provided.

Key-Words: - Closed-Loop, Optimal Control, Piezo-Electric, Internal Structure, Buck-Boost, Discontinuous Mode.

1 Introduction

With many available clean energy resources: thermal, light, vibration, etc. Energy harvesting is an active research area nowadays (see for instance [1]). However, one of the most recently focused sources is the well-known piezo-electric harvesting (see for instance [2]).

From microwatt to milliwatt, the small amount of energy harvested by a piezo-electric device must be optimized regarding it is input impedance before it can be used.

In this way, and taking into account that the internal model of a piezoelectric is far from being pure resistive, complex structures must be developed in order to extract as much energy as possible (see for instance [3]).

This optimization can be accomplished in several ways, however the following main methodologies can be considered:

- Optimal pure resistive load
- Open-loop optimal control for any load
- Closed-loop optimal control for any load

With the optimal resistive load case as the simplest possible, the other possibilities imply to find an optimal control algorithm to apply to some AC-DC converter in order to approximate, as much as possible, the well-known *maximum power transfer theorem*.

This is a very difficult hardware issue that can be approached with the use of buck-boost converters which, moreover, behave as a pure resistive input load in discontinuous mode (see [2]).

In this paper, following the research line depicted at [4], a novel optimal control technique is presented using a buck-boost converter. Starting with a buck-boost circuit connected to a rectifier bridge after the piezo-electric device, a singular optimal control strategy is developed using Pontryagin's principle.
This strategy renders the design independent of the load connected, improving and extending the applicability of energy harvesting beyond the scope of the pure resistive scenarios.
The optimal control algorithm obtained is closed-loop, so it can be readily programmed in a microprocessor. As it is well known, singular optimal control is rather more difficult than traditional non-singular optimal control.
However, this scenario allows developing a control methodology that renders the solution and switching times (bang-bang control) independent of the load.
From a practical point of view, in small PCB sizes, is required for sensor applications, the budget of external components it is an important issue.
To overcome this issue, an open-loop version, derived from the optimal closed-loop is also tested. This open-loop strategy provides a smaller amount of output power, however an adaptive circuit is implemented which shows an improvement of the power harvested.
This paper is organized as follows: Section 2 presents an internal model of a piezo-device available in the literature and the state space model of a buck-boost, Section 3 develops an optimal control law for the Buck-Boost, Section 4 uses the optimal control obtained, Section 5 presents practical implementation result of both: closed and open loop algorithms. Finally Section 6 presents some conclusions and future work.

2 Piezo-Electric's Electrical Model

A simple piezo-electric device electrical-mechanical model was considered by Van Dyke model in [8] and it is known that a piezoelectric device change the internal model when is mounted on a structure to extract energy.

This phenomenon leads the idea to consider two models instead:

- Unloaded model
- Loaded model

These models can be depicted in Figure 1.

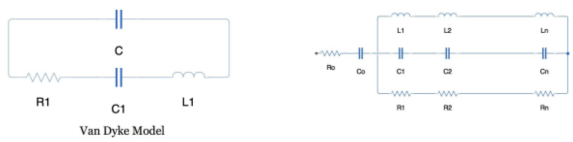

(a) Unloaded (b)Loaded

Figure 1: Van dyke's simple models at [8]

As it is well known, the physical parameter determination is not straightforward, however, some real values can found in the available literature (see for instance the model in [7] for the unloaded case (Figure 2 and Table 1).

R_0 (Ω)	5
R_1 (Ω)	115
C_0 (µf)	0.15
C_1 (mf)	0.277
L_1 (µHy)	30.253

Table 1: Parameter values of the real piezo-device given in [7]

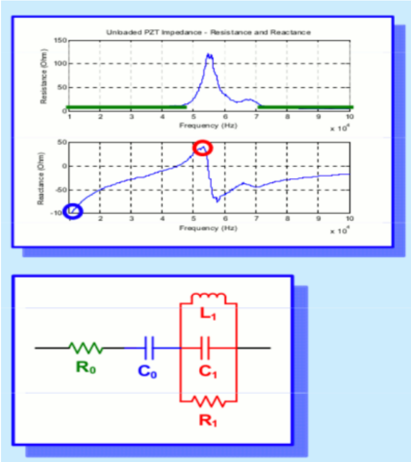

Figure 2: The model proposed in [7]

2.1 Maximum transfer power theorem

The maximum transfer power theorem reads as shown in Figure 3.

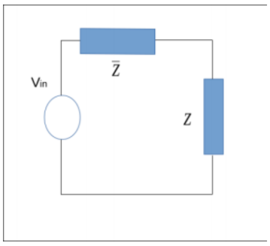

Figure 3: Maximum transfer power theorem.

where $\bar{Z}$ is the complex conjugate of Z. Neglecting the internal inductance, Figure 4 is obtained with the nominal parameters in Table 2 for the unloaded case using a pure resistive load.

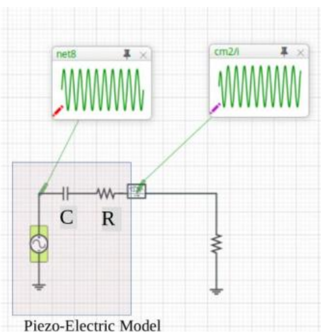

Figure 4: Piezo-device with resistive load.

R(Ω)	5
C_1 (μf)	0.13

Table 2: Piezo-device's nominal parameters neglecting inductance.

2.1.1 Pure Resistive Loads

Pure resistive loads yield low harvest power for a suboptimal load (Figure 5).

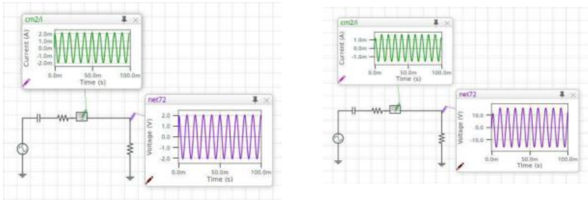

(a) R_L=1kΩ (b) R_L=10kΩ

Figure 5: Two resistive loads' simulations.

With R_L=1kΩ, P(RMS)=1mW and with R_L=10kΩ, P(RMS)=4.5mW.
The big value of the optimal load resistance would be (shaker's frequency is less than 100 Hz in typical applications):

$$R_L = \frac{1}{2 \cdot \pi \cdot f \cdot C}$$

where f the shaker's frequency. Non-resistive loads require power electronics for real applications.

2.2 The Buck-Boost topology

The Buck-Boost converter is the most common topology due to its resistive input average impedance (see [3], [6] and Figure 6).

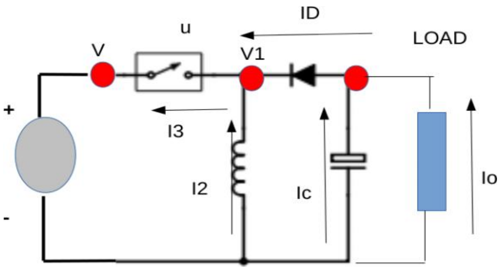

Figure 6: Buck-Boost topology

A simple analysis of the topology in Figure 6 can be depicted as follows:

Continuous Mode

$$\begin{cases} u = 0\ (Open) \Rightarrow \dfrac{dI_2}{dt} = \dfrac{V_0}{L} \\ u = 1\ (Closed) \Rightarrow \dfrac{dI_2}{dt} = \dfrac{V}{L} \end{cases}$$

Where D is the duty cycle and δ the time interval where the current runs from maximum to zero.
From these relations, the output voltage can be obtained:

$$D = \frac{V_0}{V_0 - V}$$

Discontinuous Mode

$$\begin{cases} u = 0\ (Open) \Rightarrow I_{2max} + \dfrac{V_0 \cdot \delta \cdot T_W}{L} = 0 \\ u = 1\ (Closed) \Rightarrow I_{2max} = \dfrac{V \cdot D \cdot T_W}{L} \end{cases}$$

This yield:

$$\frac{V_0}{V} = \frac{V \cdot D^2 \cdot T}{2 \cdot L \cdot I_0}$$

The stability of both continuous and discontinuous modes can be readily obtained for a fixed resistive load as explained in [11].
On the other hand, as indicated in [6], a buck-boost circuit can exhibit constant input average impedance (average voltage over average current) depending on the mode of operation as depicted in Table 3.

Discontinuous Mode	Continuous Mode
$R_{IN} = \dfrac{2 \cdot L}{D^2 \cdot T_W}$	$R_{IN} = \left(\dfrac{1-D}{D}\right)^2 \cdot R_0$

Table 3: Buck-Boost average input impedance.

with T_W the period of the switching frequency.
On the other hand, the buck-boost topology possess and inverting nature between input and output voltage (see Figure 7 simulating a piezo-device with a buck-boost and resistive load).

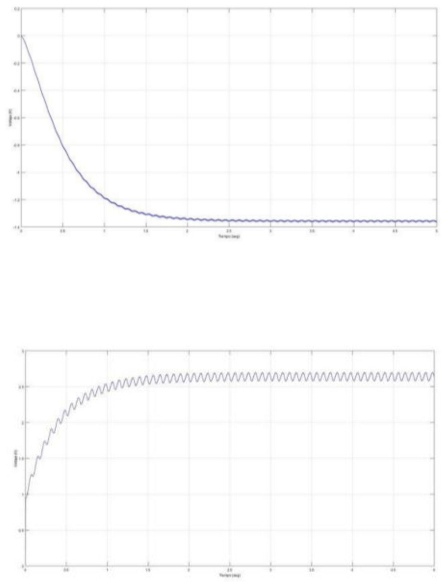

Figure 7: Buck_Boost and piezo-device simulation.

2.2.1 State-Space Model

A more detailed state-space model can be obtained considering the switch as $R^*.u$, with R^* a constant resistance along with u as in equation (2), then equation (1) is obtained:

$$\begin{gathered} F(v_1 - v_0) = C_L \cdot \dot{v_0}(t) + I_0(t) \\ \left(v_1 - v(t)\right) \cdot \left(\frac{u}{R^*}\right) = F(v_1 - v_0) + \\ -\frac{1}{L} \cdot \int v_1 \cdot d\sigma \\ v = \phi + \left[\frac{(v_1 - v) \cdot u \cdot R}{R^*} + \frac{\frac{1}{C} \cdot \int (v_1 - v) \cdot u}{R^*} \cdot d\sigma\right] \\ \phi = I(t) \cdot R + \frac{1}{C} \cdot \int I(\sigma) \cdot d\sigma \end{gathered} \quad (1)$$

Figure 8 shows the main currents and voltages with the diode model:

$$\begin{gathered} I_D = \frac{V_D}{R_D} \cdot \left(\frac{1 + sign(V_D)}{2}\right) \\ u = \{0,1\} \end{gathered} \quad (2)$$

where *sign(.)* is the well-known sign function.

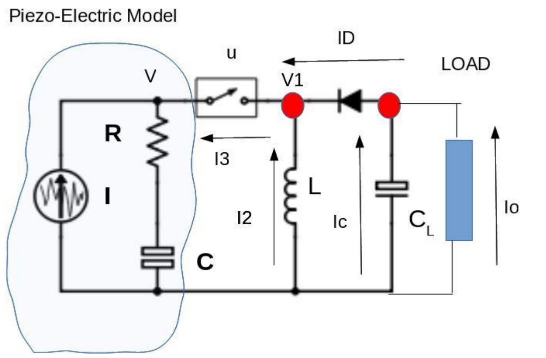

Figure 8: Electrical analysis.

The recursion in (1) must be solved:

$$\dot{x_1}(t) = \frac{1}{C_L} \cdot F(\dot{x_2} - x_1) - \frac{1}{C_L} \cdot I_0$$
$$(\dot{x_2} - \dot{x_3}) \cdot \left(\frac{u}{R^*}\right) = F(\dot{x_2} - x_1) - \frac{1}{L} \cdot x_2$$
$$\dot{x_3} = \phi(t) + (\dot{x_2} - \dot{x_3}) \cdot u \cdot \left(\frac{R}{R^*}\right) +$$
$$+ \left(\frac{u}{R^* \cdot C}\right) \cdot (x_2 - x_3)$$

to give:

$$\dot{x_2} = \varphi_1 \cdot \left(\frac{1 + sign(\varphi_1 - x_1)}{2}\right) +$$
$$\varphi_2 \cdot \left(\frac{1 + sign(\varphi_2 - x_1)}{2}\right)$$
$$-(1+u) \cdot \left(\frac{x_1}{R_D} + \frac{x_2}{L}\right) +$$
$$\varphi_1 = \frac{\frac{u}{R} \cdot (\phi + (x_2 - x_3) \cdot u)}{(1+u) \cdot \left(\frac{u}{R} - \frac{1}{R_D}\right) + u}$$
$$\varphi_2 = u \cdot R \cdot \left(\frac{-2 \cdot x_2}{L} + \frac{\phi}{R} + \frac{(x_2 - x_3)}{R}\right) +$$
$$(1-u) \cdot \left(x_1 + \frac{R_D}{L} \cdot x_2\right)$$

where: $\int_0^t x_1 = v_0, x_2 = \int_0^t v_1(\sigma) \cdot d\sigma, x_3 = \int_0^t v(\sigma) \cdot d\sigma, R = R^*$

In a compact notation:

$$\dot{x}(t) = f(x, u, I_0, \phi)$$
$$\phi = I(t) \cdot R + \frac{1}{C} \cdot \int I(\sigma) \cdot d\sigma \qquad (3)$$

with $x=[x_1,x_2,x_3]'$ and I_0 as external perturbation.

3 Optimal Control Strategy

Classical optimal control problems are formulated as follows (see for instanced [5]):

$$min_{u \in U} = \varphi(X(T)) + \int_0^T F(u,t) \cdot dt$$
$$such\ that:$$
$$\dot{x}(t) = f(x, u, \xi(t))$$
$$g(x) \leq 0$$

Where U is known as the admissible set, $\xi(t)$ is a possible external perturbation and T is a fixed time (unless $F=1$).
The particular case $F(u,t) = 0$, it is known as *singular optimal control* (see [5]).
In this way, a singular optimal control policy for the model in equation (1) in order to maximize the output power can be posed:

$$min_{u=0,1} = -x_1(t) \cdot I_0(t)$$
$$such\ that:$$
$$\dot{x}(t) = f(x, u, I_0, \phi)$$
$$(x_1 - \bar{v_0})^2 \leq \Delta_v$$

The last constraint added ensures a non-trivial solution: $x_1 \cdot I_0 = 0$ with Δ_v a constant and with $\bar{v_0}$ the desired output voltage.
Defining: $\tau \in [0,t]$, following [4], [5] pp.49-51:

- $(x_1 - v_0)^2 < \Delta v$
- $(x_1 - v_0)^2 = \Delta v$

Then:

$$min_{u=\{0,1\}}\ \lambda(t)' \cdot f(x, u, I_0, \phi)$$
$$or$$
$$(v_0 - \bar{v_0})^2 \leq \Delta v, \forall u = \{0,1\}$$

where: $\lambda(\tau = t) = \frac{\partial(x_1 \cdot I_0)}{\partial x} = [I_0, 0,0]'$.
The synthesis of the problem leads (using (3)):

$$min_{u=0,1} \frac{I_0 \cdot F(\dot{x_2} - x_1)}{C_L} \Rightarrow$$

$$u = \frac{1 - sign(I_0 \cdot (v_1 - v))}{2} \qquad (4)$$

The MATLAB/Simulink implementation is shown in Figure 9.

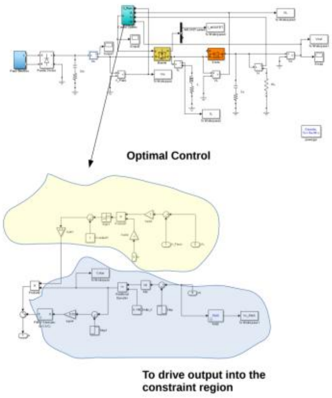

Figure 9: MATLAB/Simulink model.

The additional block forces the initial conditions inside the optimal region.

3.1 Stability analysis

The closed-loop law obtained in (4) renders the state-space model (1)-(2) a dynamical system. However, the stability of this dynamical system must be studied.
In order to accomplish this analysis, the domain of the trajectories ($\mathfrak{R}^n$) can be split in two:

- Trajectories with $(x_1 - v_0)^2 < \Delta v$
- Trajectories with $(x_1 - v_0)^2 = \Delta v$

The first case implies the optimal control acting on the buck-boost, so the output voltage remains bounded.
Moreover, the output voltage remains inside the established bounds along with (using the bounded nature of the inductance current [11]):

- $v_0 = bounded \Rightarrow v_1 = bounded\ (diode) \Rightarrow$

$$x_2 = \int_0^t v_1(\sigma) \cdot d\sigma$$

$$= bounded\ (inductance)$$

- $v = bounded\ (piezo - device) \Rightarrow x_3 = \int v\,(\sigma) \cdot d\sigma = bounded$

The state x_3 can be proved to be bounded on the basis of the input $u = \{0,1\}$:

- $u = 0 \Rightarrow\ x_3 = finite\ integral = bounded$
- $u = 1 \Rightarrow x_3 = Inductance's\ current$

The second case above implies the output voltage outside the region where the optimal control becomes active. In this case, a fixed pulse width modulation (PWM) is applied with the classical stability proved (see [11]).

4 Simulations

MATLAB/Simulink implementation it is shown in Figure 10. However, several remarks are in order:

- Domain of attraction changing with Δv
- Bigger voltage than open-loop
- Bigger output power

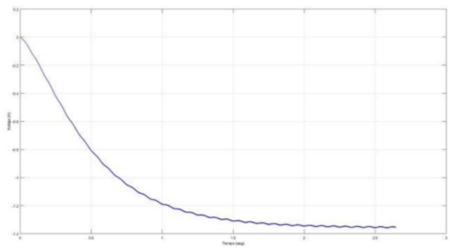

(a)

Δ_v=0.04, v_0=1.5V

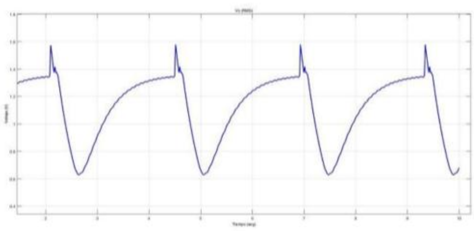

(b) Δ_v=0.15, v_0=1.5V

Figure 10: MATLAB optimal control simulation.

5 Measurements

The optimal control solution found can be implemented in closed-loop, however for the sake of future circuit simplifications, an open-loop version is going to be tested.

5.1 Closed-Loop Optimal Control

The control law thus obtained in previous sections it is straightforward implementable using a micro-controller capable of handling floating point numbers.
In this way, using the Texas' micro-controller MSP430G2253, the measurements shown in Figure 11 and Figure 12 were obtained.

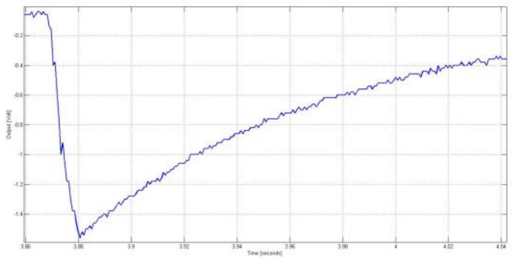

Figure 11: Output voltage's measurement with R_L=1kΩ and 0.7 G of shaker's acceleration.

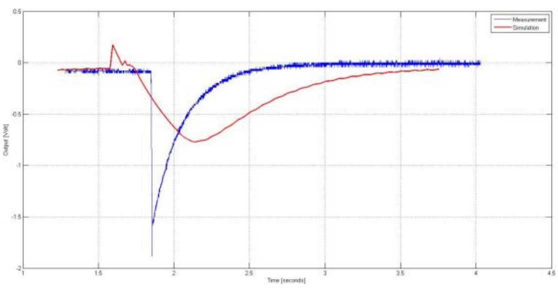

Figure 12: Output voltage's measurement with R_L=10kΩ and 0.7 G of shaker's acceleration.

It is remarkable that under 0.7 G of acceleration at 6.6 Hz of the shaker (600mV peak at the leads of the piezo-device), 1.9V (peak) is obtained at a load of 1 kΩ, this also means 1V or 1mW during 50 msecs, on the other hand, with 10 kΩ, 1V is held during 90 msecs, whereas without the optimal control this is only possible whit an excitation (acceleration) three times bigger.

The comparison with the simulations obtained at Section 4 shows that the model and the optimal control are very precise.
Both 50 msecs and 90 msecs it is enough to connect a low power micro-controller and a transmitter to use in remote applications.

5.2 Open-Loop Optimal Control

As a by-product, observing the behavior of the buck-boost output voltage, the sudden voltage increase is due to a sudden change into the PWM signal.
This conclusion leads the following open-loop optimal control strategy implemented in ENERGIA's software for a MSP430G2230 Texas' micro-controller:

```
int Out=1;
void setup() {
pinMode(P1_6, OUTPUT);}
void loop()
{
digitalWrite(P1_6,LOW);
delay(6000);
digitalWrite(P1_6,HIGH);
for(int i=0;i<100;i++)
{
if(Out= =1)
{ digitalWrite(P1_6,HIGH);
Out=0;}
else
{ digitalWrite(P1_6,LOW);
Out=1; }}}
```

Using this open-loop strategy, an obvious decrease of the output power is experienced (Figure 13).

However the use of a simpler control algorithm without the PWM function needed and with no other external components but the buck-boost, renders this idea appealing.

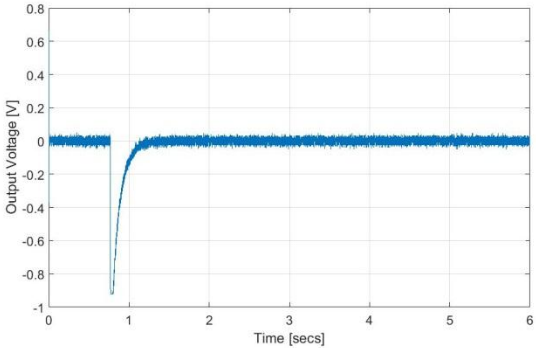

Figure 13: 1 bimorph piezo-device PFCB-W14 at 0-7 G.

On the other hand, the recent development of a mechanical device to increase the energy harvested, encourage measurements with bigger shaker accelerations (see [9]).

Following these ideas, the results in Figure 15 and Figure 16 show the non-linear increase of the output power.

To obtain deeper conclusions about the internal structure of the piezo-device and its interaction with the power electronics, an intermediate adaptive circuit is going to be tested.

This circuit takes advantage of the controlled current source in the h-parameter model of a BJT transistor and uses two piezo-electric devices, to give Figure 14 (see for instance [10]):

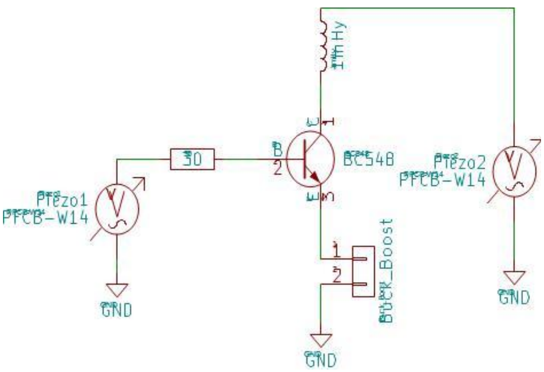

Figure 14: Adaptive circuit using 2 piezo-devices.

Finally, connecting the adaptive circuit before the buck-boost and increasing the acceleration to 2.75G, the measurement shown in Figure 15 is obtained over a load of R_L=1kΩ.

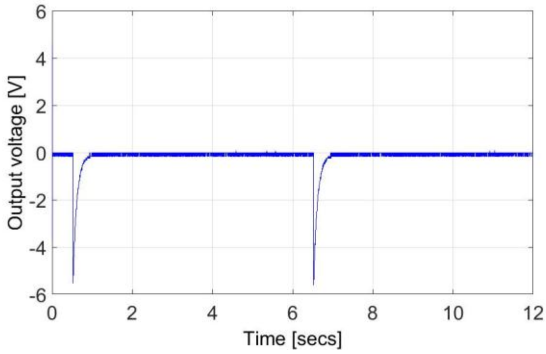

Figure 15: 2 bimorph piezo-devices PFCB-W14 without adaptive circuit.

Comparing the output power with the case of two bimorph piezo-devices in parallel without the adaptive circuit, the output power is decreased, showing the advantage to use the adaptive circuit (Figures 15 and 16).

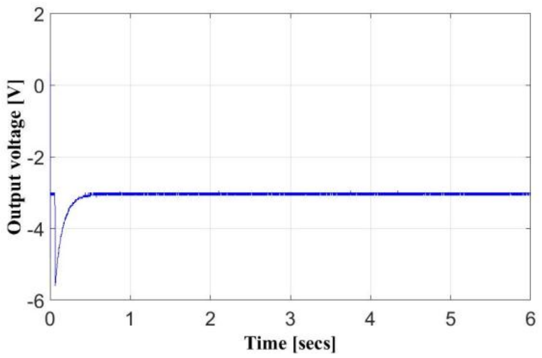

Figure 16: 2 bimorph piezo-devices PFCB-W14 with adaptive circuit.

Notice the constant value of 3V after the sudden change to 5.6V as opposed to the zero return in Figure 15.

6 Conclusions

In this paper, electric controlled power from a piezo-device using a buck-boost topology and optimal control is presented.

Starting from a simple internal model of a piezo-electric device and considering the model of every electrical component in the buck-boost circuit, and optimal control strategy is developed.

The majority of the results available in the literature consider cost functions involving integrals. In these cases, Pontryagin's principle yields the solution of ordinary differential equations known as co-state equations in order to obtain the control law.

This solution renders the input as time-varying or open-loop. In this sense, the present paper suggests a singular cost function allowing a closed-loop solution.

Considering parameters from the available literature, some simulations were presented to show the viability of the optimal control theory.

The simulations were performed with and without optimal control in MATLAB/Simulink.

In order to verify experimentally these results, some measurements were obtained to show a very big improvement in the amount of output energy.

It turns out that this closed-loop algorithm was programmed off-line in an 8-bit microcontroller becoming the result very appealing to use in remote applications were very low energy is available.

However, the external circuitry to the appropriate conditioning of the signals could result a bit involved.

This problem was overcome using an open-loop version with an intermediate adaptive circuit, showing a promising improvement of the output power when compared to the case without adaptation.

As a future work, the adaptive circuit along with the optimal control algorithm applied to a rotating mechanical structure is going to be investigated and improved.

Acknowledgements

This research was supported by Universidad Tecnológica Nacional, GIMAP under the project ENTUNBB0004269.

References:

[1] NamAdnan Harb, Energy harvesting: State-ofthe-art, *Renewable Energy: Generation and Application*, Vol.36, Issue 10, 2011, pp. 2641-2654.

[2] R. D'hulst, T. Sterken, R. Puers, G. Deconninck and J. Driesen. *Power Processing Circuits for Piezoelectric Vibration-Based energy Harvesters*, IEEE Transactions on Industrial Electronics Publishing House, Vol.57, Issue 12, 2010, pp. 4170-4177.

[3] Darmayuda I. Made, Yuan Gao San Jeow Cheng, Meng Tong Tan and Minkyu Je. *Optimum Piezoelectric Energy Harvesting, with Buck Boost Circuit in Discontinuous Conduction Mode.* International Journal of Information and Electronics Engineering, Vol. 6, 2012.

[4] Andrés García. *Singular Optimal Control Applied to DC-AC Converters.* I Congreso Argentino de Energías Sustentables, Bahía Blanca, Buenos Aires, Argentina, 2014.

[5] Hans P. Geering. *Optimal Control with Engineering Applications.* Springer, 2007.

[6] E. Lefeuvre, D. Audigier, C. Richard and D. Guyomar. *Buck-Boost Converter for Sensorless Power Optimization of Piezoelectric Energy Harvester*. IEEE Transactions on Power Electronics,Vol. 22, Number 5, pp. 2018-2025, 2007.

[7] Jina Kim, L. Griso, Jeong Kim, Dong Sam Ha and Daniel Inman. *Electrical Modeling of Piezoelectric Ceramics for Analysis and Evaluation of Sensory Systems.* IEEE Sensors Applications. Symposium, Atlanta, GA, USA. Pp. 122-127, 2008.

[8] ANSI/IEEE Std 176-1987. *IEEE Standard on Piezoelectricity.* IEEE, 1987.

[9] Machado SP, Febbo M, Gatti CD and Ramirez JM. *Non-resonant nergy harvester with elastic constraints for low rotating frequencies.* 8th Micromechanics and microsystems 2017, 23-25 August, Uppsala, Suecia.

[10] Paolo Antognetti and Giuseppe Massobrio. *Semiconductor Device Modeling with Spice.* McGraw–Hill Professional.1993.

[11] Hamed Mashinchi Mahery, Saman Torabzad, Mehran Sabahi., Ebrahim Babaei. *Modeling and stability of buck-boost dc-dc converter based on Z-transform.* (IICPE), 2012 IEEE 5th India International Conference on Power Electronics.